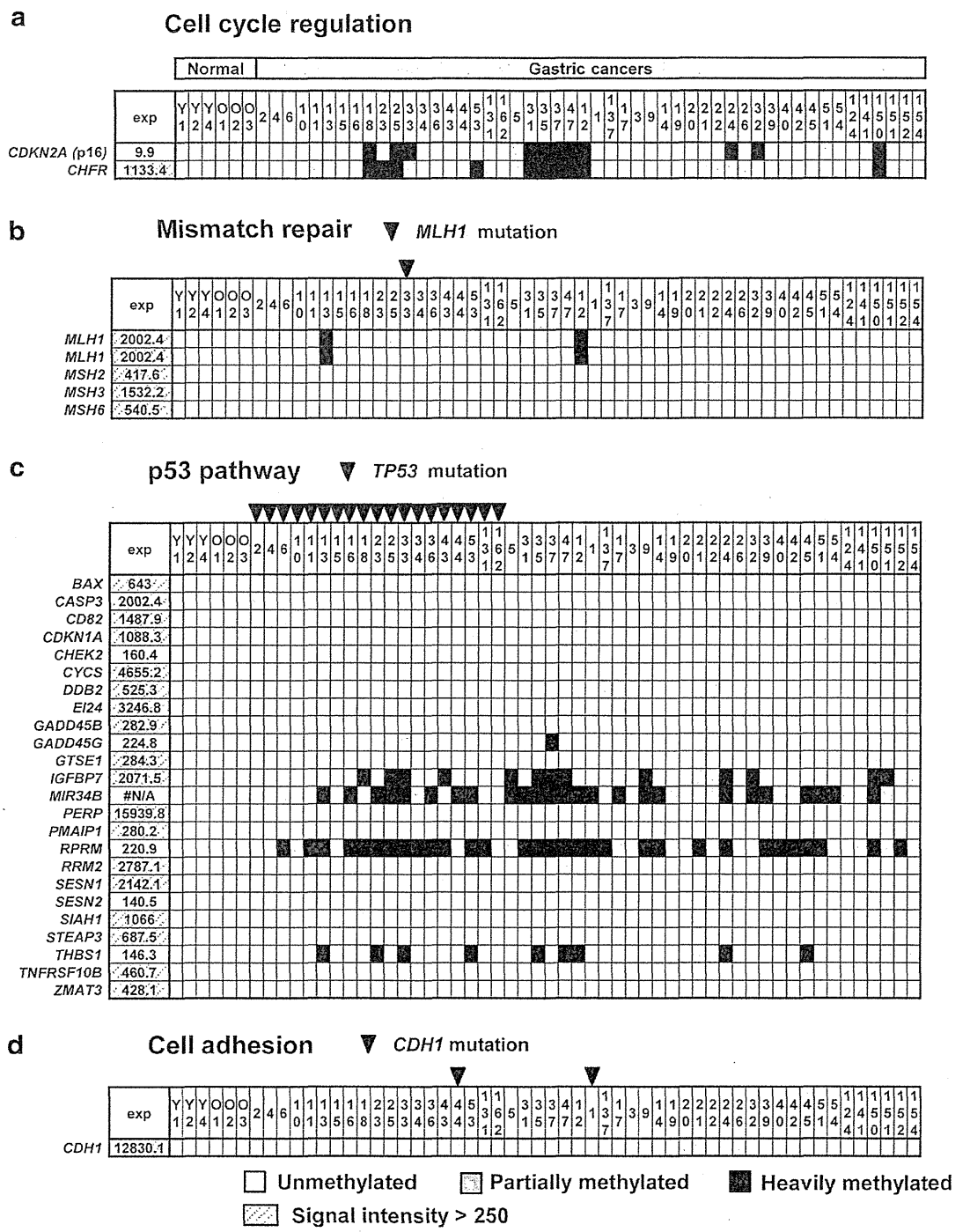

Fig. 3 Genetic and epigenetic alterations in four tumor suppressor pathways. **a** In cell-cycle regulation, none of the 50 GCs had point mutations of *CDKN2A*, whereas 13 GCs had heavy aberrant methylation of *CDKN2A* and/or *CHFR*. **b** In mismatch repair, 1 GC had a point mutation of *MLH1* (*arrowhead*), and 2 GCs had heavy aberrant methylation of *MLH1*. **c** In the p53 pathway, 19 GCs had point mutations of *TP53* (*arrowheads*), and 38 GCs had heavy aberrant methylation of 1 or more of its downstream genes. When limited to the genes with moderate or abundant expression in normal gastric mucosae (shown by *hatching*), 13 GCs had heavy aberrant methylation of *IGFBP7*. **d** In cell adhesion, 2 GCs had mutations of *CDH1* (*arrowheads*), and none of the 50 GCs had heavy aberrant methylation of *CDH1*

regulators, and 4 GCs had point mutations of *PIK3CA* or *PTPN11* (Fig. 2b). Regarding the MAPK pathway, none of the 50 GCs had aberrant methylation of its 1 negative regulator, and 11 GCs had genetic alterations of *ERBB2*, *FLT3*, or *KRAS* (Fig. 2c).

Tumor-suppressive pathways affected by epigenetic and genetic alterations

We then analyzed tumor-suppressive pathways inactivated in GCs. Regarding cell-cycle regulation, 13 of the 50 GCs had heavy aberrant methylation of *CDKN2A* and/or *CHFR*, whereas none of the 50 GCs had point mutations of *CDKN2A* (Fig. 3a). Regarding mismatch repair, 2 GCs had heavy aberrant methylation of *MLH1*, and 1 GC had a point mutation (Fig. 3b).

Regarding the p53 pathway, it is known that *TP53* itself cannot be methylation silenced because it does not have a CGI in its promoter region. However, its downstream genes with promoter CGIs could be methylation silenced. Twenty-four downstream genes had promoter CGIs and 38 GCs had heavy aberrant methylation of 1 or more of the 24 genes (Fig. 3c). Among the 24 genes, *IGFBP7* was abundantly expressed (signal intensity = 2,071.5) in normal gastric mucosae, and 13 GCs had its heavy aberrant methylation. Nineteen GCs had point mutations of *TP53*.

Regarding cell adhesion, none of the 50 GCs had heavy aberrant methylation of *CDH1*, and 9 GCs had partial aberrant methylation. At the same time, 2 GCs had its point mutations (Fig. 3d). Taken together, these results showed that genes in GC-related pathways were more frequently affected by epigenetic alterations than by genetic alterations.

Association between pathway alterations and clinicopathological characteristics

Associations between the pathway alterations and clinicopathological characteristics were analyzed using the data of 41 GCs with clinical information. First, the GCs were classified into two groups by the presence of genetic or/and epigenetic alterations of one of the seven cancer-related pathways (the WNT pathway, the AKT/mTOR pathway, the MAPK pathway, cell-cycle regulation, mismatch repair, the p53 pathway, or cell adhesion), and by that of genetic alterations of oncogenes. Then, from these classifications, those with reasonable statistical power (five or more in both groups) were selected for the clinicopathological analysis (namely, alterations of the MAPK pathway, cell-cycle regulation, and the p53 pathway, and genetic alterations of oncogenes).

As a clinicopathological factor, first, an association with prognosis was analyzed by drawing Kaplan–Meier curves using OS. The prognosis of patients with alterations of the MAPK pathway and genetic alterations of oncogenes tended to be better than that of patients without such alterations ($P = 0.166$ and 0.093, respectively; Fig. 4a,d). In contrast, alterations of cell-cycle regulation and the p53 pathway did not show any associations (Fig. 4b,c). Then, associations with other clinicopathological characteristics (gender, age, histological differentiation, depth of tumor, lymph node metastasis, and recurrence) were analyzed (Table 2). The presence of genetic alterations of oncogenes was associated with lymph node metastasis ($P = 0.021$). In contrast, alterations of the MAPK pathway, cell-cycle regulation, and the p53 pathway were not associated with any clinicopathological characteristics.

Discussion

In this study, we showed (i) that 15 and 21 of the 50 GCs had genetic alterations of oncogenes and tumor suppressor genes, respectively, and (ii) that genes in cancer-related pathways were more frequently affected by epigenetic alterations than by genetic alterations. When genetic and epigenetic alterations were combined, all the 50 GCs had alteration of cancer-related pathways. Although it is still necessary to confirm that activities of cancer-related pathways were indeed impaired by these genetic and epigenetic alterations, all the genes analyzed here were at least reported to be involved in the pathways. These pathways were considered to be potential targets for drugs.

Among the 50 GCs, some GCs had mutations and amplifications of target genes of molecular-targeted therapy. Three GCs had *ERBB2* amplifications and 4 other GCs had point mutations of genes involved in the AKT/mTOR pathway. The 3 GCs with *ERBB2* amplifications are expected to respond to trastuzumab, which was shown to improve survival of patients with *HER2* (*ERBB2*)-positive advanced GC in the ToGA trial [15]. The 4 GCs with point mutations of genes involved in the AKT/mTOR pathway might respond to everolimus, whose efficacy was shown for renal cell carcinoma [16] and breast cancer [31]. Clinical trials for GC are in progress [32, 33].

Tumor suppressor genes, such as *CDH1*, *CDKN2A*, and *MLH1*, were inactivated more frequently by epigenetic alterations than by genetic alterations. In addition, inactivation of negative regulators of the WNT pathway by epigenetic alterations was observed in all the 50 patients.

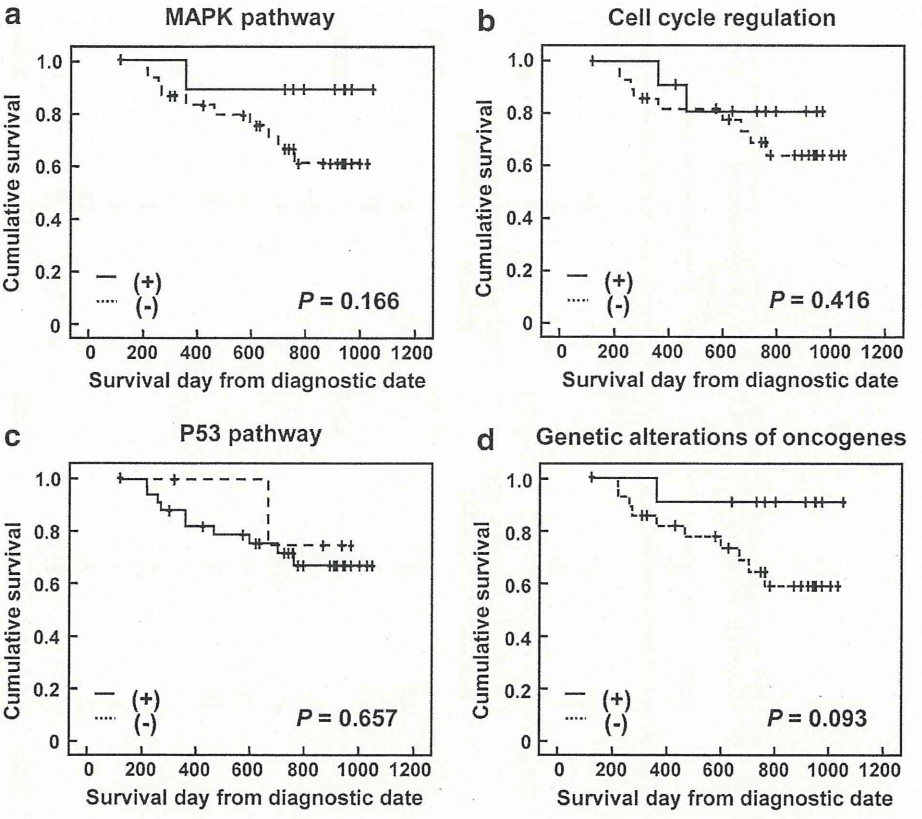

Fig. 4 Associations between a pathway alteration and patient prognosis. Kaplan–Meier curves were drawn using OS. **a** Patients with alterations of the MAPK pathway ($n = 11$) might have better prognosis than those without ($P = 0.116$). **b**, **c** The genetic or/and epigenetic alterations of cell-cycle regulation and the p53 pathway did not show any associations. **d** Patients with genetic alterations of oncogenes ($n = 12$) tended to have better prognosis than those without ($P = 0.093$)

These results showed that epigenetic alterations are deeply involved in gastric carcinogenesis. Aberrant DNA methylation can be restored by the DNA-demethylating drugs 5-azacytidine (azacitidine) and 5-aza-2′-deoxycytidine (decitabine), which are clinically used for patients with myelodysplastic syndromes [34]. Recently, clinical trials using DNA-demethylating drugs for solid tumors have been actively conducted [35], and efficacy was shown in recurrent metastatic non-small cell lung cancer [36]. There is a possibility that these epigenetic drugs are useful for the treatment of GCs.

According to a genome-wide analysis of methylated genes, several hundred to 1,000 genes whose promoter CGIs are aberrantly methylated are accumulated in cancers [37]. Expression levels of most of these genes are absent or very low in normal cells [30]. Most of them are considered not as drivers of carcinogenesis but as passengers. Therefore, we separately analyzed TSS200 CGIs of genes expressed in normal gastric mucosae. These genes are known to frequently include driver genes in carcinogenesis [38]. *DKK3* involved in the WNT pathway and *IGFBP7* involved in the p53 pathway were expressed in normal gastric mucosae and frequently methylated in GCs. It is known that downregulation of *DKK3* is correlated with tumor progression [39], and that *IGFBP7* can inhibit cell growth and induce apoptosis [40]. These results supported that aberrant methylation of *DKK3* and *IGFBP7* was involved in gastric carcinogenesis.

Patients with genetic alterations of oncogenes had a significantly smaller number of lymph nodes with metastasis than those without, and their prognosis tended to be better than those without. Although detailed mechanisms are unknown, it is known that oncogene mutations are associated with the CpG island methylator phenotype (CIMP), and that the prognosis of the CIMP(+) patients tends to be better than that of the CIMP(−) patients in GCs [23].

In conclusion, an integrated profile of genetic and epigenetic alterations of GC-related pathways was obtained using a benchtop next-generation sequencer and a bead array. The profile is expected to be useful for selection of molecular-targeted and epigenetic drugs for individual patients.

Table 2 Associations between genetic/epigenetic alterations and clinicopathological findings

Variable	*N*	Alterations of MAPK pathway		*P* value	Alterations of cell cycle regulation		*P* value	Alterations of p53 pathway		*P* value	Genetic alterations of oncogenes		*P* value
		+	−		+	−		+	−		+	−	
Gender				1.000			0.398			0.567			1.000
Male	34	8	26		9	25		29	5		10	24	
Female	7	1	6		3	4		7	0		2	5	
Age				0.743			0.101			0.436			0.451
Mean ± SD (range)		67.3 ± 11.2 (54–88)	68.8 ± 12.0 (38–88)		73.2 ± 12.2 (54–88)	66.6 ± 11.2 (38–83)		69.0 ± 11.8 (38–88)	64.6 ± 11.6 (47–76)		70.7 ± 11.7 (54–88)	67.6 ± 11.8 (38–84)	
Histological differentiation				0.231			0.494			0.146			0.278
Differentiated	14	5	9		3	11		14	0		6	8	
Undifferentiated	27	4	23		9	18		22	5		6	21	
Depth of tumor				0.088			0.370			0.852			0.230
T1	1	0	1		1	0		1	0		1	0	
T2	9	4	5		2	7		9	0		4	5	
T3	14	4	10		3	11		12	2		4	10	
T4	17	1	16		6	11		14	3		3	14	
Lymph node metastasis				0.070			0.524			0.173			0.021
N0	6	3	3		3	3		6	0		4	2	
N1	7	3	4		1	6		6	1		3	4	
N2	10	1	9		2	8		7	3		0	10	
N3	18	2	16		6	12		17	1		5	13	
Recurrence				0.441			0.305			1.000			0.084
Negative	25	7	18		9	16		22	3		10	15	
Positive	16	2	14		3	13		14	2		2	14	

Depth of tumor and lymph node metastasis are based on the 7th edition tumor-node-metastasis classification of the International Union Against Cancer

Acknowledgments Y.Y. is a recipient of Research Resident Fellowships from the Foundation for Promotion of Cancer Research. This work was supported by the National Cancer Center Research and Development Fund, by a Grant-in-Aid for the Third-term Comprehensive Cancer Control Strategy from the Ministry of Health, Labour and Welfare, by a Grant-in-Aid for Scientific Research from Japan Society for the Promotion of Science (JSPS), and by the A3 Foresight Program from the Japan Society for the Promotion of Science.

Conflict of interest The authors have declared that no competing interests exist.

References

1. Ushijima T. Detection and interpretation of altered methylation patterns in cancer cells. Nat Rev Cancer. 2005;5:223–31.
2. Maekita T, Nakazawa K, Mihara M, Nakajima T, Yanaoka K, Iguchi M, et al. High levels of aberrant DNA methylation in *Helicobacter pylori*-infected gastric mucosae and its possible association with gastric cancer risk. Clin Cancer Res. 2006;12:989–95.
3. Nojima M, Suzuki H, Toyota M, Watanabe Y, Maruyama R, Sasaki S, et al. Frequent epigenetic inactivation of SFRP genes and constitutive activation of Wnt signaling in gastric cancer. Oncogene. 2007;26:4699–713.
4. Yu J, Tao Q, Cheng YY, Lee KY, Ng SS, Cheung KF, et al. Promoter methylation of the Wnt/beta-catenin signaling antagonist Dkk-3 is associated with poor survival in gastric cancer. Cancer (Phila). 2009;115:49–60.
5. Taniguchi H, Yamamoto H, Hirata T, Miyamoto N, Oki M, Nosho K, et al. Frequent epigenetic inactivation of Wnt inhibitory factor-1 in human gastrointestinal cancers. Oncogene. 2005;24:7946–52.
6. Vivanco I, Sawyers CL. The phosphatidylinositol 3-kinase AKT pathway in human cancer. Nat Rev Cancer. 2002;2:489–501.
7. Byun DS, Lee MG, Chae KS, Ryu BG, Chi SG. Frequent epigenetic inactivation of RASSF1A by aberrant promoter hypermethylation in human gastric adenocarcinoma. Cancer Res. 2001;61:7034–8.
8. Sun Y, Deng D, You WC, Bai H, Zhang L, Zhou J, et al. Methylation of p16 CpG islands associated with malignant transformation of gastric dysplasia in a population-based study. Clin Cancer Res. 2004;10:5087–93.
9. Kang GH, Lee S, Cho NY, Gandamihardja T, Long TI, Weisenberger DJ, et al. DNA methylation profiles of gastric carcinoma characterized by quantitative DNA methylation analysis. Lab Invest. 2008;88:161–70.
10. Duval A, Hamelin R. Mutations at coding repeat sequences in mismatch repair-deficient human cancers: toward a new concept of target genes for instability. Cancer Res. 2002;62:2447–54.
11. Qu Y, Dang S, Hou P. Gene methylation in gastric cancer. Clin Chim Acta. 2013;424:53–65.
12. Guilford P, Hopkins J, Harraway J, McLeod M, McLeod N, Harawira P, et al. E-cadherin germline mutations in familial gastric cancer. Nature (Lond). 1998;392:402–5.
13. Machado JC, Oliveira C, Carvalho R, Soares P, Berx G, Caldas C, et al. E-cadherin gene (CDH1) promoter methylation as the second hit in sporadic diffuse gastric carcinoma. Oncogene. 2001;20:1525–8.
14. Oue N, Oshimo Y, Nakayama H, Ito R, Yoshida K, Matsusaki K, et al. DNA methylation of multiple genes in gastric carcinoma: association with histological type and CpG island methylator phenotype. Cancer Sci. 2003;94:901–5.
15. Bang YJ, Van Cutsem E, Feyereislova A, Chung HC, Shen L, Sawaki A, et al. Trastuzumab in combination with chemotherapy versus chemotherapy alone for treatment of HER2-positive advanced gastric or gastro-oesophageal junction cancer (ToGA): a phase 3, open-label, randomised controlled trial. Lancet. 2010;376:687–97.
16. Motzer RJ, Escudier B, Oudard S, Hutson TE, Porta C, Bracarda S, et al. Phase 3 trial of everolimus for metastatic renal cell carcinoma: final results and analysis of prognostic factors. Cancer (Phila). 2010;116:4256–65.
17. Rohle D, Popovici-Muller J, Palaskas N, Turcan S, Grommes C, Campos C, et al. An inhibitor of mutant IDH1 delays growth and promotes differentiation of glioma cells. Science. 2013;340:626–30.
18. Geutjes EJ, Bajpe PK, Bernards R. Targeting the epigenome for treatment of cancer. Oncogene. 2012;31:3827–44.
19. Delmore JE, Issa GC, Lemieux ME, Rahl PB, Shi J, Jacobs HM, et al. BET bromodomain inhibition as a therapeutic strategy to target c-Myc. Cell. 2011;146:904–17.
20. Dawson MA, Prinjha RK, Dittmann A, Giotopoulos G, Bantscheff M, Chan WI, et al. Inhibition of BET recruitment to chromatin as an effective treatment for MLL-fusion leukaemia. Nature (Lond). 2011;478:529–33.
21. Gullapalli RR, Lyons-Weiler M, Petrosko P, Dhir R, Becich MJ, LaFramboise WA. Clinical integration of next-generation sequencing technology. Clin Lab Med. 2012;32:585–99.
22. Dedeurwaerder S, Defrance M, Calonne E, Denis H, Sotiriou C, Fuks F. Evaluation of the Infinium methylation 450K technology. Epigenomics. 2010;3:771–84.
23. Kim JG, Takeshima H, Niwa T, Rehnberg E, Shigematsu Y, Yoda Y, et al. Comprehensive DNA methylation and extensive mutation analyses reveal an association between the CpG island methylator phenotype and oncogenic mutations in gastric cancers. Cancer Lett. 2013;330:33–40.
24. Shigematsu Y, Niwa T, Yamashita S, Taniguchi H, Kushima R, Katai H, et al. Identification of a DNA methylation marker that detects the presence of lymph node metastases of gastric cancers. Oncol Lett. 2012;4:268–74.
25. Teschendorff AE, Marabita F, Lechner M, Bartlett T, Tegner J, Gomez-Cabrero D, et al. A beta-mixture quantile normalization method for correcting probe design bias in Illumina Infinium 450k DNA methylation data. Bioinformatics. 2013;29:189–96.
26. Jones PA, Baylin SB. The epigenomics of cancer. Cell. 2007;128:683–92.
27. Lin JC, Jeong S, Liang G, Takai D, Fatemi M, Tsai YC, et al. Role of nucleosomal occupancy in the epigenetic silencing of the MLH1 CpG island. Cancer Cell. 2007;12:432–44.
28. Ball MP, Li JB, Gao Y, Lee JH, LeProust EM, Park IH, et al. Targeted and genome-scale strategies reveal gene-body methylation signatures in human cells. Nat Biotechnol. 2009;27:361–8.
29. Parsonnet J, Friedman GD, Vandersteen DP, Chang Y, Vogelman JH, Orentreich N, et al. *Helicobacter pylori* infection and the risk of gastric carcinoma. N Engl J Med. 1991;325(16):1127–31.
30. Takeshima H, Yamashita S, Shimazu T, Niwa T, Ushijima T. The presence of RNA polymerase II, active or stalled, predicts epigenetic fate of promoter CpG islands. Genome Res. 2009;19:1974–82.
31. Beaver JA, Park BH. The BOLERO-2 trial: the addition of everolimus to exemestane in the treatment of postmenopausal hormone receptor-positive advanced breast cancer. Future Oncol. 2012;8:651–7.
32. Lee SJ, Lee J, Park SH, Park JO, Park YS, Lim HY, et al. Phase II trial of capecitabine and everolimus (RAD001) combination in refractory gastric cancer patients. Invest New Drugs. 2013;31:1580–6.
33. Yoon DH, Ryu MH, Park YS, Lee HJ, Lee C, Ryoo BY, et al. Phase II study of everolimus with biomarker exploration in

patients with advanced gastric cancer refractory to chemotherapy including fluoropyrimidine and platinum. Br J Cancer. 2012;106:1039–44.
34. Kantarjian H, Issa JP, Rosenfeld CS, Bennett JM, Albitar M, DiPersio J, et al. Decitabine improves patient outcomes in myelodysplastic syndromes: results of a phase III randomized study. Cancer (Phila). 2006;106:1794–803.
35. Nebbioso A, Carafa V, Benedetti R, Altucci L. Trials with 'epigenetic' drugs: an update. Mol Oncol. 2012;6:657–82.
36. Juergens RA, Wrangle J, Vendetti FP, Murphy SC, Zhao M, Coleman B, et al. Combination epigenetic therapy has efficacy in patients with refractory advanced non-small cell lung cancer. Cancer Discov. 2011;1:598–607.
37. Yamashita S, Hosoya K, Gyobu K, Takeshima H, Ushijima T. Development of a novel output value for quantitative assessment in methylated DNA immunoprecipitation-CpG island microarray analysis. DNA Res. 2009;16:275–86.
38. Kikuyama M, Takeshima H, Kinoshita T, Okochi-Takada E, Wakabayashi M, Akashi-Tanaka S, et al. Development of a novel approach, the epigenome-based outlier approach, to identify tumor-suppressor genes silenced by aberrant DNA methylation. Cancer Lett. 2012;322:204–12.
39. Yue W, Sun Q, Dacic S, Landreneau RJ, Siegfried JM, Yu J, et al. Downregulation of Dkk3 activates beta-catenin/TCF-4 signaling in lung cancer. Carcinogenesis. 2008;29:84–92.
40. Ruan W, Xu E, Xu F, Ma Y, Deng H, Huang Q, et al. IGFBP7 plays a potential tumor suppressor role in colorectal carcinogenesis. Cancer Biol Ther. 2007;6:354–9.

Oncogene (2013), 1–6

www.nature.com/onc

SHORT COMMUNICATION

ANGPTL4 is a secreted tumor suppressor that inhibits angiogenesis

E Okochi-Takada[1], N Hattori[1], T Tsukamoto[2], K Miyamoto[3], T Ando[1,4], S Ito[5], Y Yamamura[5], M Wakabayashi[1], Y Nobeyama[1,6] and T Ushijima[1]

Tumor suppressors with extracellular function are likely to have advantages as targets for cancer therapy, but few are known. Here, we focused on angiopoietin-like 4 (ANGPTL4), which is a secreted glycoprotein involved in lipoprotein metabolism and angiogenesis, is methylation-silenced in human cancers, but has unclear roles in cancer development and progression. We found a deletion mutation in its coiled-coil domain at its N-terminal in human gastric cancers, in addition to hypermethylation of the *ANGPTL4* promoter CpG islands. Forced expression of wild-type *ANGPTL4*, but not *ANGPTL4* with the deletion, at physiological levels markedly suppressed *in vivo* tumorigenicity and tumor angiogenesis, indicating that the latter caused the former. Tumor-derived ANGPTL4 suppressed *in vitro* vascular tube formation and proliferation of human umbilical vascular endothelial cells, partly due to suppression of ERK signaling. These showed that ANGPTL4 is a genetically and epigenetically inactivated secreted tumor suppressor that inhibits tumor angiogenesis.

Oncogene advance online publication, 20 May 2013; doi:10.1038/onc.2013.174

Keywords: epigenetics; angiogenesis; tumor suppressor; gastric cancer; DNA methylation

INTRODUCTION

Tumor-suppressor genes (TSGs) are somatically inactivated by genetic and/or epigenetic mechanisms.[1,2] Targeting TSGs for molecular target therapy has been attempted mainly for *p53*.[3,4] However, the attempts have not been easy, partly due to the fact that the *p53* gene product is neither a cell surface protein nor a typical enzyme.[5] Considering efficient delivery to targets, TSGs whose products function extracellularly as secreted proteins are likely to have advantages. So far, secreted frizzled-related proteins are known as secreted tumor suppressors,[6,7] but few others are known.

As a candidate, we previously identified that angiopoietin-like 4 (*ANGPTL4*), a member of the angiopoietin-like family, was silenced by aberrant DNA methylation of promoter CpG islands (CGIs) (methylation-silenced) in human cancers.[8,9] ANGPTL4 is a secreted glycoprotein, and is involved in lipoprotein metabolism through inhibition of lipoprotein lipase.[10] In contrast, the role of ANGPTL4 in angiogenesis remains controversial.[11–15] Likewise, its role in tumor formation also remains controversial—some reports suggesting its tumor-suppressive function[12,16,17] and others its oncogenic function.[18–20]

Here, we aimed to clarify the role of ANGPTL4 in cancer development and progression and also in tumor angiogenesis.

RESULTS AND DISCUSSION

Inactivation of *ANGPTL4* by epigenetic and genetic mechanisms in human gastric cancers

ANGPTL4 methylation was detected in 10 of 91 human gastric cancers (11%) by quantitative real-time methylation-specific PCR (Figure 1a). The mRNA and protein expression levels of ANGPTL4 in cancers with *ANGPTL4* methylation were significantly lower than those in cancers without methylation (Supplementary Figure S2). Methylation status did not have any association with clinicopathological features, but had a significant association with Epstein-Barr virus infection status and the presence of the CGI methylator phenotype[21] (Supplementary Figure S1 and Supplementary Table S1). In non-cancerous gastric mucosae of 71 gastric cancer patients and gastric mucosae of 58 healthy volunteers, the methylation level was also quantified. It was significantly higher in cancer patients than in healthy volunteers and in individuals with *H. pylori* infection than in those without (Figure 1b). This suggested the potential involvement of *ANGPTL4* methylation in the formation of an epigenetic field for cancerization, a predisposed normal-appearing tissue.[22]

ANGPTL4 mutation was then analyzed in 89 of the 91 gastric cancers (due to sample availability), and a somatic 21-bp deletion in exon 1 was identified in one specimen (cancer #217T) without *ANGPTL4* methylation (Figures 1c and d). ANGPLT4 consists of an N-terminal coiled-coil domain (CCD) and a C-terminal fibrinogen-like domain,[23,24] and the 21-bp deletion was located in the CCD (Supplementary Figure S3). The CCD is reported to be critical for regulation of the anti-angiogenic activity of ANGPTL4,[13] and the deletion here involved one of the two cysteine residues (Cys76 and Cys80) essential for the activity regulation by oligomerization.[25,26]

Loss of heterozygosity (LOH), which suggests the presence of a TSG,[27] was detected in 4 of 16 samples (25%) informative for a C/T polymorphism at the second position of codon 266. The locus of

[1]Division of Epigenomics, National Cancer Center Research Institute, Tokyo, Japan; [2]Oncological Pathology Division, Aichi Cancer Center Research Institute, Nagoya, Japan; [3]Division of Molecular Oncology, National Hospital Organization Kure Medical Center and Chugoku Cancer Center, Kureshi, Japan; [4] Third Department of Internal Medicine, University of Toyama, Toyama, Japan; [5]Department of Gastroenterological Surgery, Aichi Cancer Center Central Hospital, Nagoya, Japan and [6]Department of Dermatology, The Jikei University School of Medicine, Tokyo, Japan. Correspondence: Dr T Ushijima, Division of Epigenomics, National Cancer Center Research Institute, 5-1-1 Tsukiji, Chuo-ku, Tokyo 104-0045, Japan.
E-mail: tushijim@ncc.go.jp
Received 27 September 2012; revised 14 February 2013; accepted 28 March 2013

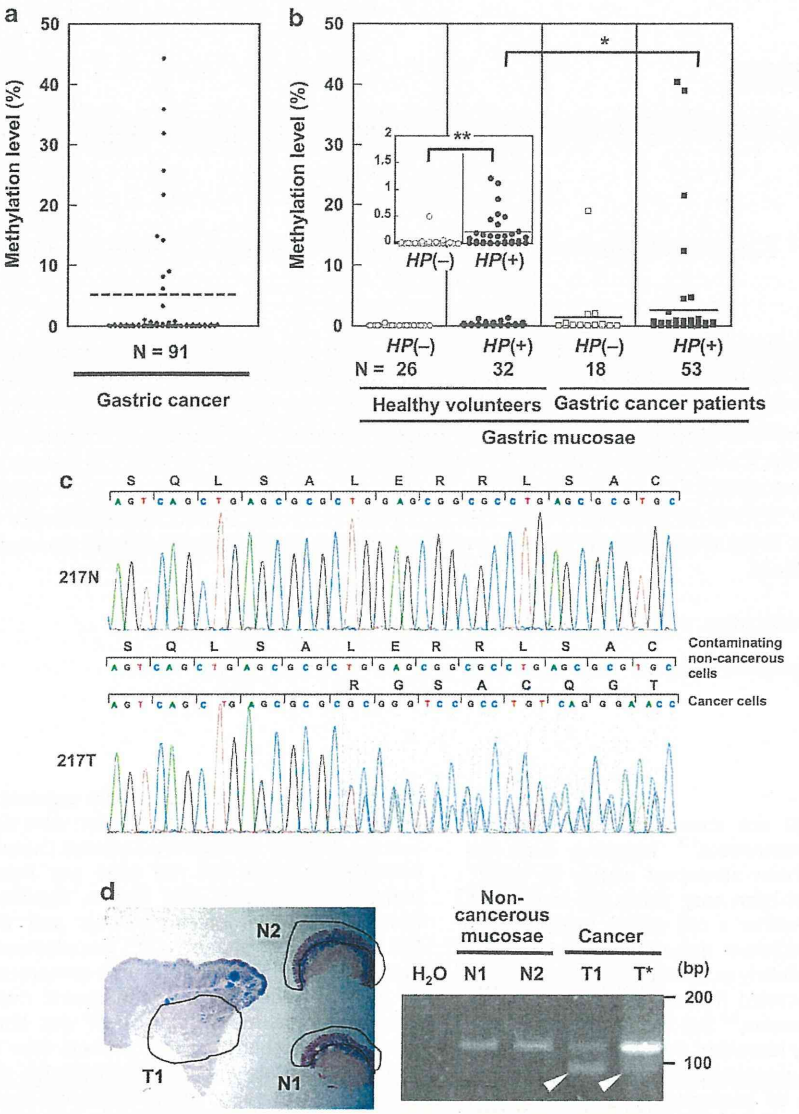

Figure 1. Aberrant methylation and a mutation of *ANGPTL4* in human gastric cancers, and methylation in non-cancerous gastric mucosae. (**a**) *ANGPTL4* methylation levels in gastric cancer specimens. Cancer samples were obtained from 91 gastric cancer patients undergoing gastrectomy with informed consents and approval by the institutional review boards. Some of the samples and methylation data were obtained from our previous study.[33] Quantitative real-time methylation-specific PCR was conducted with sodium bisulfite-treated DNA and primer sets specific to methylated and unmethylated sequences (Supplementary Table S2). Using a cutoff value of 6% (broken line), as in previous studies,[34–36] 10 cancer specimens were considered to have aberrant methylation. (**b**) *ANGPTL4* methylation levels in gastric mucosae of 58 healthy volunteers (30 male and 28 female; average age = 55 years) and 71 non-cancerous gastric mucosae of gastric cancer patients (50 male and 21 female; average age = 67 years) obtained by endoscopic biopsy of the antral region. *H. pylori* infection status was analyzed by a serum anti-*H. pylori* IgG antibody test (SRL, Tokyo, Japan), rapid urease test (Otsuka, Tokushima, Japan) or culture test (Eiken, Tokyo, Japan). The methylation level in gastric mucosae was significantly higher in gastric cancer patients than in healthy volunteers. The mean methylation level is shown by a horizontal line. $^{*}P<0.05$, $^{**}P<0.01$ (the unpaired Welch's *t*-test, two-sided). (**c**) A deletion mutation in a human gastric cancer specimen. All the seven exons and splice donor/acceptor sites of *ANGPTL4* were amplified by PCR (Supplementary Table S2), and the PCR products were directly cycle sequenced. The sequences of a gastric cancer specimen (217T) and its corresponding non-cancerous tissue (217N) between nucleotides 385 and 423 are shown. A 21-bp deletion in exon 1 was detected (shown in the gray background). (**d**) Confirmation of the deletion mutation using DNA samples obtained from a single tissue section. A 117-bp region encompassing the deletion was amplified by PCR, and the deletion was detected as a PCR product with a shorter size (96 bp). DNA from the cancer (T1), but not that from non-cancerous areas (N1 and N2), yielded the shorter product (shown by arrows). T*, genomic DNA extracted from frozen tumor tissues. If LOH was present in T1, the band intensity ratio was expected to be 1:1 (wild type:deletion mutant) (fraction of cancer cells was pathologically assessed to be 61–67%). If LOH was not present, it was expected to be 2:1. The ratio observed was ~1:2, and LOH was considered to be present in T1.

ANGPTL4, 19p13.3, has been suggested to contain TSGs, due to frequent LOH of the region in several types of cancers, such as pancreatic and colon cancers.[28–30] In addition, two human gastric cancer cell lines (MKN28 and AGS) without *ANGPTL4* expression had methylation of its promoter, and their treatment with 5-aza-2′-deoxycytidine (5-aza-dC), a DNA methylation inhibitor,

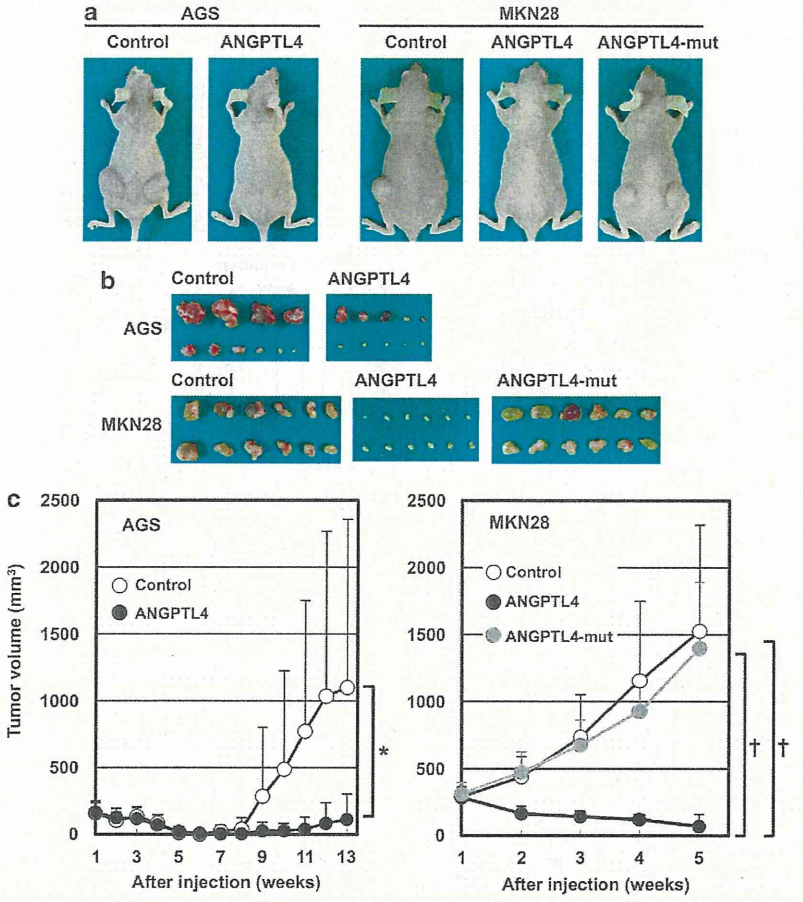

Figure 2. The effect of *ANGPTL4* and its mutant with the 21-bp deletion on tumor formation. The complementary DNA of wild-type *ANGPTL4*, its mutant with the deletion, and *EGFP* as a control were inserted into a mammalian expression vector pIRESpuro3 with the human cytomegalovirus immediate early promoter (Clontech, Mountain View, CA, USA). Individual vectors were transfected into MKN28 or AGS gastric cancer cell lines, and transfectants were selected with puromycin (0.3 μg/ml). Athymic nude mice (BALB/cAJc1-nu/nu, CLEA, Tokyo, Japan) were subcutaneously injected with cells (1×10^7 cells) mixed with an equal volume of Matrigel (BD Biosciences, San Diego, CA, USA). All the animal experiments were approved by the Committee for Ethics in Animal Experimentation, and conducted in accordance with the Guidelines for Animal Experiments of the National Cancer Center. (**a**) Representative photographs of transplanted tumors at 13 weeks (AGS) and 5 weeks (MKN28). *ANGPTL4* markedly suppressed tumor formation, while its mutant with the deletion lacked the activity. (**b**) Macroscopic views of the tumors resected at 13 weeks (AGS) and at 5 weeks (MKN28). Introduction of *ANGPTL4* markedly suppressed tumor sizes in both cell lines. The variable degree of suppression in AGS might have been due to the lower ANGPTL4 expression level (Supplementary Figure S5c). (**c**) Tumor growth curves after the injection. The volume of tumor (mm^3) was calculated by the formula: (length × $width^2$)/2. A tumor volume is shown as a mean ± s.d. ($N = 10$ in AGS and $N = 12$ in MKN28). $^*P < 0.05$, $^\dagger P < 0.001$ (Student's *t*-test).

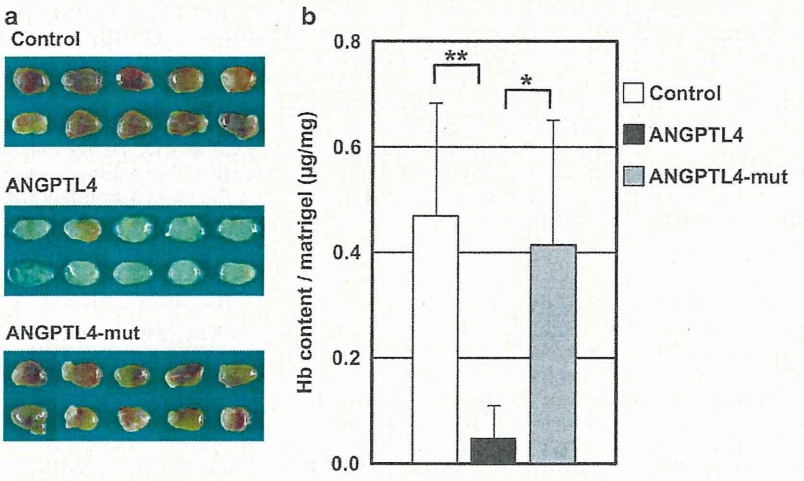

Figure 3. For caption see next page.

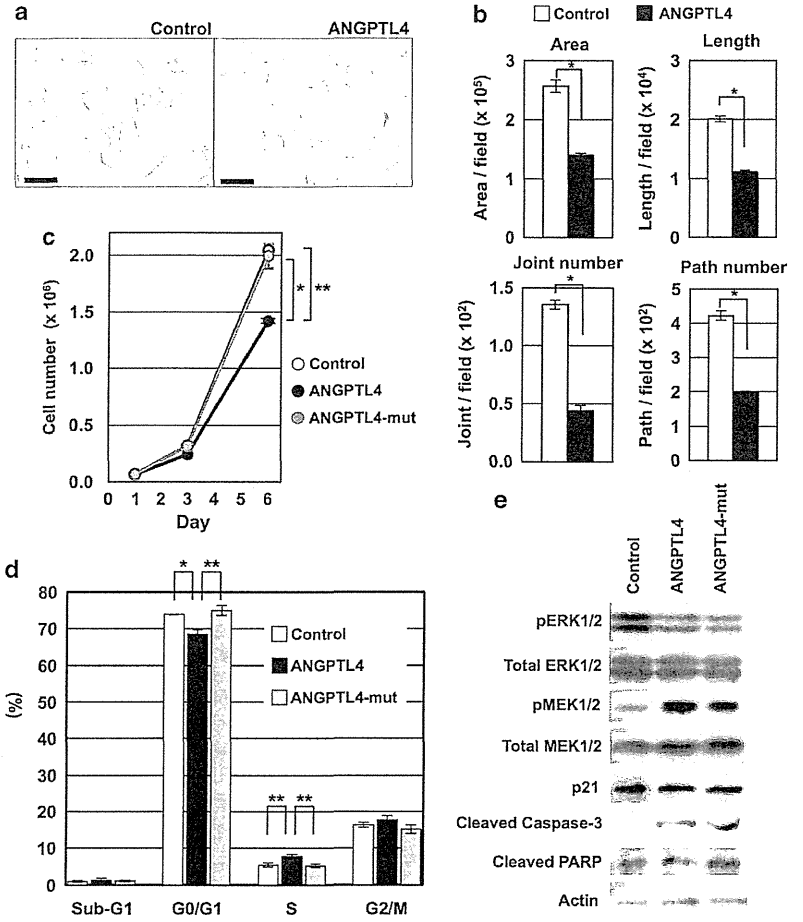

Figure 4. *In vitro* anti-angiogenic activity of tumor-derived ANGPTL4 and its molecular mechanisms. (**a**) Suppression of vascular tube formation by ANGPTL4. A conditioned medium was prepared by mixing the medium of subconfluent MKN28 cells expressing control or *ANGPTL4* and the HUVEC medium with VEGF-A (10 ng/ml) at 1:2. HUVECs on feeder neonatal normal human dermal fibroblast cells (Angiogenesis Kit, Kurabo, Osaka, Japan) arrived from the manufacturer on day 0, and the conditioned medium was supplemented on days 1, 4, 7 and 9. On day 11, cells were fixed and endothelial tubes were stained with anti-CD31antibody (BD Pharmingen, San Diego, CA, USA). The experiment was conducted in triplicate. Scale bars, 50 μm. (**b**) Quantification of the extent of vascular tube formation. Four parameters were scored in nine visual fields per well using the angiogenesis quantification software (Kurabo), and all the four parameters were shown to be suppressed by ANGPTL4. The results are shown as a mean ± s.d. $*P<0.001$ (Student's *t*-test). (**c**) Suppression of the HUVEC growth by ANGPTL4, but not by its mutant with the deletion. HUVECs were seeded at a density of 1×10^5 cells/10-cm dish on day 0, and the conditioned medium prepared as in **a** was supplemented on days 1, 3 and 5. The number of cells was counted on day 3 and day 6 by a Countess Automated Cell Counter (Invitrogen, Carlsbad, CA, USA). Each culture was carried out three times, and the result is shown as a mean ± s.d. $*P=8.4\times10^{-4}$, $**P=5.5\times10^{-5}$ (Student's *t*-test). (**d**) The effects of ANGPTL4 and its mutant with the deletion on the cell cycle of HUVECs. The HUVECs on day 6 of **c** were stained with propidium iodide, and cell populations in different phases of the cell cycle were determined by a FACS Caliber flow cytometer (Becton Dickinson, San Diego, CA). S-phase arrest was observed in HUVECs exposed to ANGPTL4, but not to its mutant with the deletion. $*P<0.05$, $**P<0.01$ (Student's *t*-test). (**e**) Immunoblot analysis of various signal molecules in HUVECs on day 6 of **c**. Decrease of pERK1/2 and increase of pMEK1/2 were induced by ANGPTL4 and also by its mutant with the deletion. This was considered because the deletion mutation affected mainly the interaction between ANGPTL4 and extracellular matrix, which was not necessary for this analysis. Primary antibodies used include anti-phospho-ERK1/2 (1:100, Cell Signaling Technology, Danvers, MA, USA), anti-total ERK1/2 (1:100, Cell Signaling Technology), anti-phospho-MEK1/2 (1:1000, Cell Signaling Technology), anti-total MEK1/2 (1:100, Cell Signaling Technology), anti-p21 (1:200, Cell Signaling Technology), anti-cleaved Caspase-3 (Asp175) (1:200, Cell Signaling Technology), anti-cleaved PARP (Asp214) (1:200, Cell Signaling Technology) and anti-actin (1:1000, Santa Cruz Biotechnology, Santa Cruz, CA, USA). Secondary antibodies conjugated to horseradish peroxidase were obtained from Cell Signaling Technology.

Figure 3. Inhibition of tumor angiogenesis by *ANGPTL4*, but not by its mutant with the deletion. (**a**) Macroscopic view of the Matrigel plugs recovered in the Matrigel plug assay. Matrigel (Matrigel basement membrane matrix high concentration, phenol red-free, BD Biosciences) was mixed with the MKN28 cells (5×10^6 cells) expressing control, *ANGPTL4*, or its mutant with the deletion. The Matrigel plug was subcutaneously injected into 5-week-old female athymic nude mice on day 1, and was recovered on day 10. Marked inhibition of tumor angiogenesis by *ANGPTL4*, but not by its mutant with the deletion, was observed. Brown color shows infiltration of blood vessels into the Matrigel plugs. (**b**) Hemoglobin content in the Matrigel plugs ($N=10$). The plugs were homogenized in red blood cell-lysing buffer (Sigma-Aldrich, St Louis, MO, USA), and the supernatants were measured with Drabkin's reagent (Sigma-Aldrich) to quantify the hemoglobin content in the plug. The content is shown as a mean ± s.d. ($N=10$). $*P=8.0\times10^{-4}$, $**P=1.2\times10^{-4}$ (Student's *t*-test).

demethylated the promoter and restored the *ANGPTL4* expression (Supplementary Figure S4). This showed methylation silencing of *ANGPTL4* in these cell lines.

Marked suppression of *in vivo* tumor growth by ANGPTL4, but not by a mutant with the deletion

The function of ANGPTL4, along with its mutant with the deletion, was examined by stably introducing wild-type or mutant *ANGPTL4* complementary DNA into MKN28 and AGS. The expression levels of the exogenous wild-type *ANGPTL4* and its mutant were kept in the range comparable to its physiological expression in gastric mucosae (Supplementary Figure S5a), and expression of *ANGPTL4* with the deletion mutation was confirmed by the amplification of a shorter size fragment (Supplementary Figure S5b).

Regarding *in vitro* effects, the *ANGPTL4* expression did not affect cell morphology, motility or cell growth (Supplementary Figures S6–S8). However, *in vivo*, sizes of engrafted tumors were strikingly suppressed by the wild-type *ANGPTL4*, markedly in AGS and almost completely in MKN28 (Figure 2). In contrast, when the mutant *ANGPTL4* was expressed in MKN28, it did not show any anti-tumorigenic effect. The presence of ANGPTL4 mRNA and protein expression in the transplanted tumors was confirmed (Supplementary Figures S9 and S10). The role of *ANGPTL4* in tumor development and progression has been highly controversial, but our data clearly showed that *ANGPTL4* suppresses tumor formation, at least in gastric cancers.

Inhibition of tumor angiogenesis as a mechanism for tumor suppression

As a mechanism for tumor suppression by *ANGPTL4*, anti-angiogenic activity of tumor-derived ANGPTL4 was examined. We performed an *in vivo* Matrigel plug angiogenesis assay to observe the vascularization that invades into a Matrigel[31] using MKN28 cells with control (*EGFP*), *ANGPTL4*, and its mutant with the deletion. Ten days after subcutaneous transplantation, the Matrigel plugs containing the control cells showed a high degree of blood vessel recruitment, as visualized by the high content of hemoglobin (Figure 3) and by the staining of CD31-positive vascular endothelial cells (Supplementary Figure S11). In contrast, the Matrigel plugs containing the *ANGPTL4*-expressing cells showed a marked suppression of the blood vessel recruitment. However, *ANGPTL4* with the deletion mutation did not have such activity. The lack of the suppressive effect was in accordance with a report that the CCD was essential for the interaction with the extracellular matrix and for its *in vivo* suppressive activity.[13] These results strongly indicated that the marked anti-angiogenic activity of tumor-derived ANGPTL4 was the cause of the marked suppression of tumor growth by ANGPTL4.

Mechanisms for the anti-angiogenic activity of the tumor-derived ANGPTL4

The mechanisms of how tumor-derived, secreted ANGPTL4 exerts its anti-angiogenic effect were analyzed. First, we conducted a vascular tube formation assay using human umbilical vein endothelial cells (HUVECs). A conditioned medium from *ANGPTL4*-expressing cells suppressed vascular tube formation of HUVECs, as visualized by staining with anti-CD31antibody (Figure 4a), and all the parameters to assess vascular formation were markedly suppressed (Figure 4b). This result showed that a large part of the anti-angiogenic activity of tumor-derived ANGPTL4 was mediated by the suppression of vascular tube formation in the tumor microenvironment.

The effect of the conditioned medium on the growth of HUVECs was then analyzed. The conditioned medium from cells expressing *ANGPTL4*, but not that from cells expressing its mutant with the deletion, suppressed the growth (Figure 4c). Cell cycle analysis showed that the conditioned medium from *ANGPTL4*-expressing cells significantly increased the number of cells in the S phase, suggesting that it induced an S-phase arrest (Figure 4d). However, the amount of p21, a potential inducer of the S-phase arrest,[32] was not increased (Figure 4e). No induction of apoptosis was observed by western blot analysis of apoptosis-related proteins, cleaved Caspase-3 and cleaved PARP (Figure 4e), or by terminal deoxynucleotidyl transferase dUTP nick end labeling (TUNEL) assay (Supplementary Figure S8).

Finally, the effect of tumor-derived ANGPTL4 on the MAPK signaling was analyzed. The conditioned medium from the *ANGPTL4*-expressing cells clearly inhibited the phosphorylation of ERK1/2 (pERK1/2) (Figure 4e), and the phosphorylation of its immediate upstream mediator, pMEK, was in contrast increased. The conditioned medium from the cells expressing the mutant with the deletion showed a similar activity to that of the *ANGPTL4*-expressing cells. As CCD is not important for the delivery to target cells *in vitro* and the fibrinogen-like domain is important for inhibition of the Raf/MEK/ERK signaling,[11] it was considered that the deletion mutation did not affect the inhibition activity.

This study demonstrated that *ANGPTL4* is a mutated and methylation-silenced tumor suppressor whose product is secreted and inhibits angiogenesis. *ANGPTL4* mutation (loss-of-function) was identified for the first time in any type of cancers, and the anti-angiogenic activity of tumor-derived ANGPTL4 was shown here also for the first time. These data warrant further research into utilizing ANGPTL4 as a target of anti-angiogenesis cancer therapy.

CONFLICT OF INTEREST

The authors declare no conflict of interest.

ACKNOWLEDGEMENTS

We are grateful to Dr Masabumi Shibuya, Tokyo Medical and Dental University, for his expert advice. This study was supported by the Third-term Comprehensive Cancer Control Strategy from the Ministry of Health, Labour and Welfare, Japan and by National Cancer Center Research and Development Fund. YN is a recipient of a Research Resident Fellowships from the Foundation for Promotion of Cancer Research.

REFERENCES

1 Knudson AG. Two genetic hits (more or less) to cancer. *Nat Rev Cancer* 2001; **1**: 157–162.
2 Baylin SB, Jones PA. A decade of exploring the cancer epigenome - biological and translational implications. *Nat Rev Cancer* 2011; **11**: 726–734.
3 Kishore R, Losordo DW. Gene therapy for restenosis: biological solution to a biological problem. *J Mol Cell Cardiol* 2007; **42**: 461–468.
4 Lane DP, Cheok CF, Lain S. p53-based cancer therapy. *Cold Spring Harb Perspect Biol* 2010; **2**: a001222.
5 Levine AJ, Oren M. The first 30 years of p53: growing ever more complex. *Nat Rev Cancer* 2009; **9**: 749–758.
6 Suzuki H, Watkins DN, Jair KW, Schuebel KE, Markowitz SD, Chen WD *et al.* Epigenetic inactivation of *SFRP* genes allows constitutive WNT signaling in colorectal cancer. *Nat Genet* 2004; **36**: 417–422.
7 Shi Y, He B, You L, Jablons DM. Roles of secreted frizzled-related proteins in cancer. *Acta Pharmacol Sin* 2007; **28**: 1499–1504.
8 Kaneda A, Kaminishi M, Yanagihara K, Sugimura T, Ushijima T. Identification of silencing of nine genes in human gastric cancers. *Cancer Res* 2002; **62**: 6645–6650.
9 Hattori N, Okochi-Takada E, Kikuyama M, Wakabayashi M, Yamashita S, Ushijima T. Methylation silencing of angiopoietin-like 4 in rat and human mammary carcinomas. *Cancer Sci* 2011; **102**: 1337–1343.
10 Miida T, Hirayama S. Impacts of angiopoietin-like proteins on lipoprotein metabolism and cardiovascular events. *Curr Opin Lipidol* 2010; **21**: 70–75.
11 Yang YH, Wang Y, Lam KS, Yau MH, Cheng KK, Zhang J *et al.* Suppression of the Raf/MEK/ERK signaling cascade and inhibition of angiogenesis by the carboxyl terminus of angiopoietin-like protein 4. *Arterioscler Thromb Vasc Biol* 2008; **28**: 835–840.

12 Ito Y, Oike Y, Yasunaga K, Hamada K, Miyata K, Matsumoto S *et al.* Inhibition of angiogenesis and vascular leakiness by angiopoietin-related protein 4. *Cancer Res* 2003; **63**: 6651–6657.
13 Chomel C, Cazes A, Faye C, Bignon M, Gomez E, Ardidie-Robouant C *et al.* Interaction of the coiled-coil domain with glycosaminoglycans protects angiopoietin-like 4 from proteolysis and regulates its antiangiogenic activity. *FASEB J* 2009; **23**: 940–949.
14 Hermann LM, Pinkerton M, Jennings K, Yang L, Grom A, Sowders D *et al.* Angiopoietin-like-4 is a potential angiogenic mediator in arthritis. *Clin Immunol* 2005; **115**: 93–101.
15 Ma T, Jham BC, Hu J, Friedman ER, Basile JR, Molinolo A *et al.* Viral G protein-coupled receptor up-regulates Angiopoietin-like 4 promoting angiogenesis and vascular permeability in Kaposi's sarcoma. *Proc Natl Acad Sci USA* 2010; **107**: 14363–14368.
16 Li KQ, Li WL, Peng SY, Shi XY, Tang HL, Liu YB. Anti-tumor effect of recombinant retroviral vector-mediated human ANGPTL4 gene transfection. *Chin Med J (Engl)* 2004; **117**: 1364–1369.
17 Galaup A, Cazes A, Le Jan S, Philippe J, Connault E, Le Coz E *et al.* Angiopoietin-like 4 prevents metastasis through inhibition of vascular permeability and tumor cell motility and invasiveness. *Proc Natl Acad Sci USA* 2006; **103**: 18721–18726.
18 Padua D, Zhang XH, Wang Q, Nadal C, Gerald WL, Gomis RR *et al.* TGFbeta primes breast tumors for lung metastasis seeding through angiopoietin-like 4. *Cell* 2008; **133**: 66–77.
19 Zhu P, Tan MJ, Huang RL, Tan CK, Chong HC, Pal M *et al.* Angiopoietin-like 4 protein elevates the prosurvival intracellular O_2^-:H_2O_2 ratio and confers anoikis resistance to tumors. *Cancer Cell* 2011; **19**: 401–415.
20 Nakayama T, Hirakawa H, Shibata K, Abe K, Nagayasu T, Taguchi T. Expression of angiopoietin-like 4 in human gastric cancer: ANGPTL4 promotes venous invasion. *Oncol Rep* 2010; **24**: 599–606.
21 Issa JP. CpG island methylator phenotype in cancer. *Nat Rev Cancer* 2004; **4**: 988–993.
22 Ushijima T. Epigenetic field for cancerization. *J Biochem Mol Biol* 2007; **40**: 142–150.
23 Hato T, Tabata M, Oike Y. The role of angiopoietin-like proteins in angiogenesis and metabolism. *Trends Cardiovasc Med* 2008; **18**: 6–14.
24 Oike Y, Akao M, Kubota Y, Suda T. Angiopoietin-like proteins: potential new targets for metabolic syndrome therapy. *Trends Mol Med* 2005; **11**: 473–479.
25 Ge H, Yang G, Huang L, Motola DL, Pourbahrami T, Li C. Oligomerization and regulated proteolytic processing of angiopoietin-like protein 4. *J Biol Chem* 2004; **279**: 2038–2045.
26 Yin W, Romeo S, Chang S, Grishin NV, Hobbs HH, Cohen JC. Genetic variation in ANGPTL4 provides insights into protein processing and function. *J Biol Chem* 2009; **284**: 13213–13222.
27 Mei R, Galipeau PC, Prass C, Berno A, Ghandour G, Patil N *et al.* Genome-wide detection of allelic imbalance using human SNPs and high-density DNA arrays. *Genome Res* 2000; **10**: 1126–1137.
28 Hoglund M, Gorunova L, Andren-Sandberg A, Dawiskiba S, Mitelman F, Johansson B. Cytogenetic and fluorescence in situ hybridization analyses of chromosome 19 aberrations in pancreatic carcinomas: frequent loss of 19p13.3 and gain of 19q13.1-13.2. *Genes Chromosomes Cancer* 1998; **21**: 8–16.
29 Trojan J, Brieger A, Raedle J, Esteller M, Zeuzem S. 5′-CpG island methylation of the *LKB1/STK11* promoter and allelic loss at chromosome 19p13.3 in sporadic colorectal cancer. *Gut* 2000; **47**: 272–276.
30 Sobottka SB, Haase M, Fitze G, Hahn M, Schackert HK, Schackert G. Frequent loss of heterozygosity at the 19p13.3 locus without *LKB1/STK11* mutations in human carcinoma metastases to the brain. *J Neurooncol* 2000; **49**: 187–195.
31 Tanner JE, Forte A, Panchal C. Nucleosomes bind fibroblast growth factor-2 for increased angiogenesis *in vitro* and *in vivo*. *Mol Cancer Res* 2004; **2**: 281–288.
32 Zhu H, Zhang L, Wu S, Teraishi F, Davis JJ, Jacob D *et al.* Induction of S-phase arrest and p21 overexpression by a small molecule 2[[3-(2,3-dichlorophenoxy) propyl] amino]ethanol in correlation with activation of ERK. *Oncogene* 2004; **23**: 4984–4992.
33 Asada K, Ando T, Niwa T, Nanjo S, Watanabe N, Okochi-Takada E *et al. FHL1* on chromosome X is a single-hit gastrointestinal tumor-suppressor gene and contributes to the formation of an epigenetic field defect. *Oncogene* 2012; **32**: 2140–2149.
34 Ando T, Yoshida T, Enomoto S, Asada K, Tatematsu M, Ichinose M *et al.* DNA methylation of microRNA genes in gastric mucosae of gastric cancer patients: its possible involvement in the formation of epigenetic field defect. *Int J Cancer* 2009; **124**: 2367–2374.
35 Enomoto S, Maekita T, Tsukamoto T, Nakajima T, Nakazawa K, Tatematsu M *et al.* Lack of association between CpG island methylator phenotype in human gastric cancers and methylation in their background non-cancerous gastric mucosae. *Cancer Sci* 2007; **98**: 1853–1861.
36 Ota N, Kawakami K, Okuda T, Takehara A, Hiranuma C, Oyama K *et al.* Prognostic significance of $p16^{INK4a}$ hypermethylation in non-small cell lung cancer is evident by quantitative DNA methylation analysis. *Anticancer Res* 2006; **26**: 3729–3732.

Supplementary Information accompanies this paper on the Oncogene website (http://www.nature.com/onc)

OPEN ACCESS Freely available online

PLOS ONE

Estimation of the Fraction of Cancer Cells in a Tumor DNA Sample Using DNA Methylation

Takamasa Takahashi[1,5,6], Yasunori Matsuda[1,2], Satoshi Yamashita[1], Naoko Hattori[1], Ryoji Kushima[3], Yi-Chia Lee[4], Hiroyasu Igaki[5], Yuji Tachimori[5], Masato Nagino[6], Toshikazu Ushijima[1*]

1 Division of Epigenomics, National Cancer Center Research Institute, Tokyo, Japan, **2** Department of Gastroenterological Surgery, Graduate School of Medicine, Osaka City University, Osaka, Japan, **3** Pathology and Clinical Laboratory Division, National Cancer Center Hospital, Tokyo, Japan, **4** Department of Internal Medicine, College of Medicine, National Taiwan University, Taipei, Taiwan, **5** Esophageal Surgery Division, National Cancer Center Hospital, Tokyo, Japan, **6** Division of Surgical Oncology, Department of Surgery, Nagoya University Graduate School of Medicine, Nagoya, Japan

Abstract

Contamination of normal cells is almost always present in tumor samples and affects their molecular analyses. DNA methylation, a stable epigenetic modification, is cell type-dependent, and different between cancer and normal cells. Here, we aimed to demonstrate that DNA methylation can be used to estimate the fraction of cancer cells in a tumor DNA sample, using esophageal squamous cell carcinoma (ESCC) as an example. First, by an Infinium HumanMethylation450 BeadChip array, we isolated three genomic regions (*TFAP2B*, *ARHGEF4*, and *RAPGEFL1*) i) highly methylated in four ESCC cell lines, ii) hardly methylated in a pooled sample of non-cancerous mucosae, a pooled sample of normal esophageal mucosae, and peripheral leukocytes, and iii) frequently methylated in 28 ESCCs (*TFAP2B*, 24/28; *ARHGEF4*, 20/28; and *RAPGEFL1*, 19/28). Second, using eight pairs of cancer and non-cancer cell samples prepared by laser capture microdissection, we confirmed that at least one of the three regions was almost completely methylated in ESCC cells, and all the three regions were almost completely unmethylated in non-cancer cells. We also confirmed that DNA copy number alterations of the three regions in 15 ESCC samples were rare, and did not affect the estimation of the fraction of cancer cells. Then, the fraction of cancer cells in a tumor DNA sample was defined as the highest methylation level of the three regions, and we confirmed a high correlation between the fraction assessed by the DNA methylation fraction marker and the fraction assessed by a pathologist ($r=0.85$; $p<0.001$). Finally, we observed that, by correction of the cancer cell content, CpG islands in promoter regions of tumor-suppressor genes were almost completely methylated. These results demonstrate that DNA methylation can be used to estimate the fraction of cancer cells in a tumor DNA sample.

Citation: Takahashi T, Matsuda Y, Yamashita S, Hattori N, Kushima R, et al. (2013) Estimation of the Fraction of Cancer Cells in a Tumor DNA Sample Using DNA Methylation. PLoS ONE 8(12): e82302. doi:10.1371/journal.pone.0082302

Editor: Qian Tao, The Chinese University of Hong Kong, Hong Kong

Received June 6, 2013; **Accepted** October 22, 2013; **Published** December 2, 2013

Funding: This study was supported by the Third-term Comprehensive Cancer Control Strategy from the Ministry of Health, Labour and Welfare, Japan (http://www.mhlw.go.jp), and by Project for Development of Innovative Research on Cancer Therapeutics (P-DIRECT) from the Ministry of Education, Culture Sports, Science, and Technology, Japan (http://p-direct.mext.go.jp). T.T. and Y.M. are recipients of a Research Resident Fellowship from the Foundation for Promotion of Cancer Research (http://www.fpcr.or.jp). The funders had no role in study design, data collection and analysis, decision to publish, or preparation of the manuscript.

Competing interests: The authors have declared that no competing interests exist.

* E-mail: tushijim@ncc.go.jp

Introduction

Contamination of normal cells, such as normal epithelial cells, fibroblasts, and peripheral leukocytes, is almost always present in tumor samples. Such contamination influences the results of cancer genome analyses [1-4], and RNA expression analysis [5,6]. If the fraction of cancer cells in a tumor DNA sample can be readily assessed, we can conduct more accurate analysis by excluding samples with extremely low tumor cell content, and by normalizing the raw data based upon the fraction of cancer cells. Traditionally, a fraction of cancer cells in a tumor sample has been assessed by pathological analysis using neighboring sections. However, preparation of such sections is sometimes difficult or impossible due to sample availability, and, above all, expert pathologists are necessary for such analysis.

To overcome these issues, technologies to estimate a fraction of cancer cells were recently developed using single nucleotide polymorphism (SNP) microarray and next generation sequencing (NGS) [7-10]. With SNP microarray, the fraction of cancer cells can be calculated by detecting genomic regions with copy number alterations and measuring the degree of allelic imbalance using SNPs in the genomic regions [7-9]. With NGS, tumor-specific mutations can be identified,

and the fraction of cancer cells can be calculated based upon the mutant allele frequency [10]. Since these technologies were originally developed for the analysis of SNPs or mutations, they suffer from complicated calculation formulae, expensive reagents, and the necessity of analysing paired normal samples.

DNA methylation is a stable epigenetic modification, and some genomic regions are methylated in a cell type-dependent manner [11-13]. Between cancer and normal cells, many genomic regions are reported to be differentially methylated in many types of cancers, and some of them are causally involved in cancer development and progression [14-18]. Among such differentially methylated genomic regions, some specific genomic regions may be completely methylated in cancer cells but yet completely unmethylated in normal cells, such as normal epithelial cells, fibroblasts, and peripheral leukocytes. If so, DNA methylation levels of the specific genomic regions can reflect the fraction of cancer cells in a sample (Figure 1A), and such estimation of the fraction of cancer cells using DNA methylation can become a useful method for cancer studies.

In this study, we aimed to demonstrate that DNA methylation could be used as a fraction marker for the estimation of a fraction of cancer cells in a tumor DNA sample, using esophageal squamous cell carcinoma (ESCC) samples as an example. To this end, we conducted a genome-wide methylation analysis to search specific genomic regions completely methylated in ESCC cells and completely unmethylated in various normal cells.

Materials and Methods

Ethics Statement

This study was conducted with the approval of the Institutional Review Board of the National Cancer Center Hospital, the Osaka City University Hospital, and the National Taiwan University Hospital. Written informed consents were obtained from all individuals.

Samples and ESCC Cell Lines

A total of 160 ESCC samples were collected at the National Cancer Center Hospital, the Osaka City University Hospital, and the National Taiwan University Hospital. The 160 ESCC samples consisted of 39 biopsy samples and 121 surgical specimens. The biopsy samples were derived from 39 patients who underwent endoscopic biopsy and were diagnosed to have an ESCC (33 male and 6 female; average age = 63, range = 30–78). Samples were stored in RNAlater (Applied Biosystems, Foster City, CA, USA) at -80 °C. The surgical specimens were derived from 121 patients who were diagnosed to have a histologically invasive ESCC and had undergone esophagectomy (98 male and 23 female; average age = 65, range = 41–82). Among the 121 surgical specimens, 25 specimens were obtained from samples embedded in paraffin wax block after fixation with formalin or 70% ethanol, and the other 96 specimens were obtained from samples stored in RNAlater (Applied Biosystems) after resection. Additionally, laser capture microdissection (LCM) was performed for eight surgical specimens embedded in paraffin wax block using LM200 (Arcturus, Mount View, CA, USA) as described [19].

Four ESCC cell lines KYSE30, KYSE50, KYSE220, and KYSE270 [20] were purchased from Health Science Research Resources Bank (Osaka, Japan). Genomic DNA was extracted by using the phenol/chloroform method.

Genome-wide DNA Methylation Analysis

Genome-wide screening of differentially methylated CpG sites was performed using an Infinium HumanMethylation450 BeadChip array, which covered 482,421 CpG sites (Illumina, San Diego, CA, USA) as described previously [21]. 11,551 CpG sites on the sex chromosomes were excluded, and the remaining 470,870 CpG sites were used for the analysis. The methylation level of each CpG site was represented by a β value, which ranged from 0 (completely unmethylated) to 1 (completely methylated).

Methylation-sensitive High Resolution Melting Analysis (MS-HRMA)

For MS-HRMA, first, 1 μg of DNA digested with *Bam*HI was treated with sodium bisulfite and suspended in 40 μL of TE buffer as described [22]. Second, PCR was conducted using 1 μL aliquot of the sodium bisulfite-treated DNA, primers capable of amplifying both methylated and unmethylated DNA (Table S1) [23], SYBR Green I (BioWhittaker Molecular Applications, Rockland, MD, USA), and an iCycler Thermal Cycler (Bio-Rad Laboratories, CA, USA). Third, HRMA of the PCR product was conducted to obtain the melting profile of the PCR product by plotting the negative derivative of fluorescence over temperature ($-dF/dT$ vs. T), using the iCycler Thermal Cycler software (Bio-Rad Laboratories, Ver. 2.1). Finally, the methylation level of a sample was assessed by comparison of its melting profile with those of fully methylated and unmethylated controls, along with mixtures of 0, 20, 40, 60, 80, and 100% methylated controls. As a fully methylated control, genomic DNA treated with *Sss*I methylase (New England Biolabs, Beverly, MA, USA) was used. As a fully unmethylated control, sodium bisulfite-modified DNAs obtained from non-cancerous esophageal mucosae without methylation of the analyzed regions was used.

Genomic DNA Copy Number Analysis

Copy number alterations of the genomic regions were analyzed by quantitative real-time PCR using an iCycler Thermal Cycler (Bio-Rad Laboratories) with SYBR green I (BioWhittaker Molecular Applications). The number of DNA molecules in a sample was measured for three regions flanking the candidate genes and control genes [*ALB* (4q13.3), *GAPDH* (12p13) and *KCNA1* (12p13.32)] located on chromosomal regions with infrequent copy number alterations. The primer sequences are shown in Table S2. The number of DNA molecules of the three candidate genes was normalized to those of the control genes. The normalized number of DNA molecules in a sample was compared with that in human leukocyte DNA to obtain copy number alterations. All the analysis was conducted in triplicate. Significant copy number

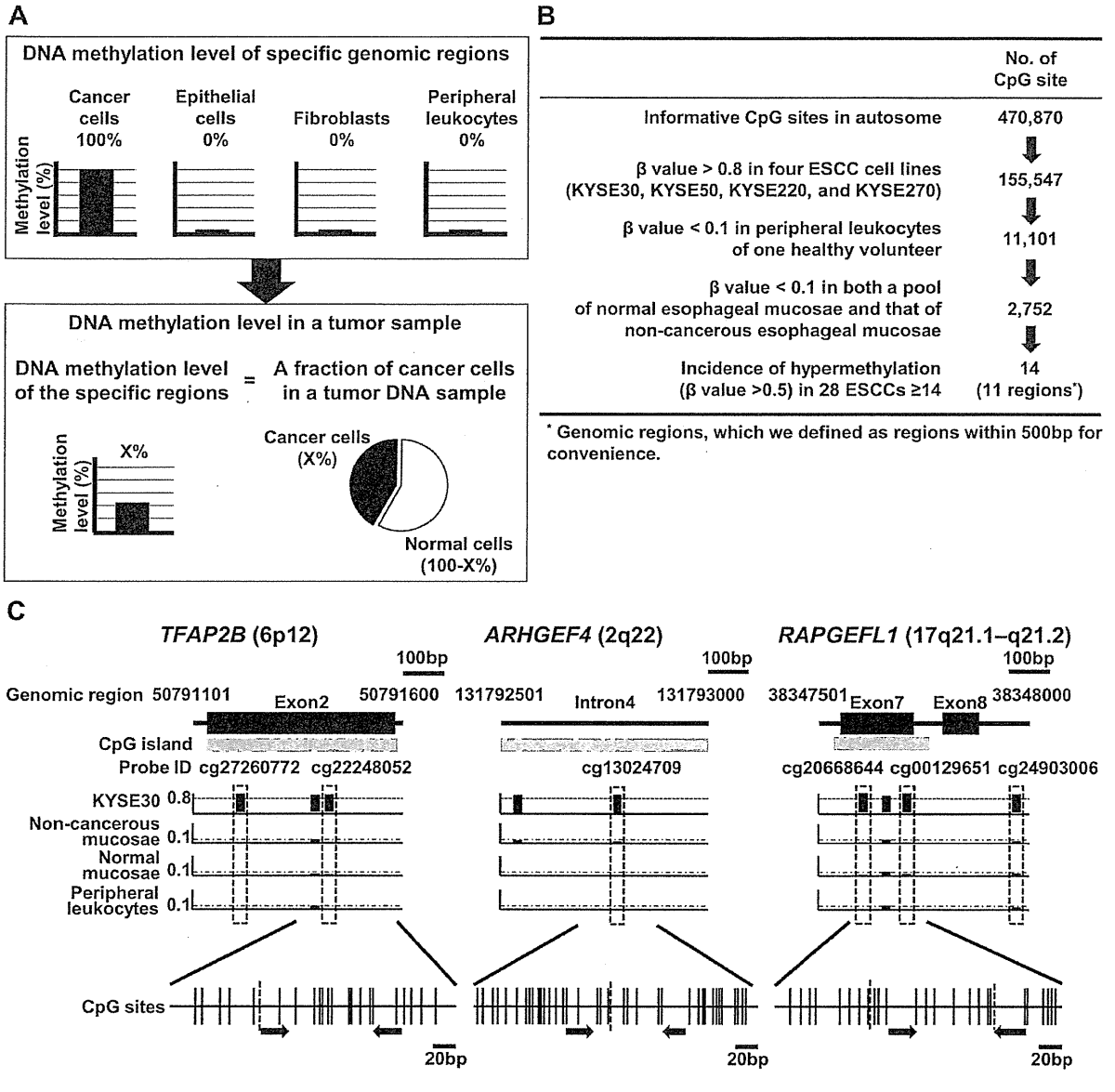

Figure 1

Figure 1. Selection processes of specific genomic regions. (A) The concept of estimation of the fraction of cancer cells in a tumor DNA sample using DNA methylation. (B) Selection of specific genomic regions, which were completely methylated in ESCC cells and completely unmethylated in various normal cells, by genome-wide methylation analysis using an Infinium HumanMethylation450 BeadChip array. Fourteen CpG sites were finally selected, and those were derived from 11 genomic regions. (C) Three genomic regions (TFAP2B, *ARHGEF4*, and *RAPGEFL1*) selected as components of a fraction marker. Gene structure and the location of a CpG island are shown at the top, and the β values of the CpG sites analyzed by the Infinium bead array are shown. The CpG site identified by the Infinium bead array is boxed by a rectangle with a dotted line. A CpG map around the CpG site(s) identified is shown at the bottom. Vertical lines (solid and broken) show CpG sites and broken lines show CpG sites whose β values were measured by the bead array. Closed arrows show primers for MS-HRMA.

doi: 10.1371/journal.pone.0082302.g001

Table 1. Genomic regions identified by beadchip analysis.

No.	Gene symbol	Gene name	Chr	nt, number	Probe ID	Relation to CpG island	Position to gene	Incidence[a]
1	*TFAP2B***	Transcription factor AP-2 beta	6	50791202	cg27260772	Island	Body	24
				50791419	cg22248052	Island	Body	14
2	*SOX2OT*	SOX2 overlapping transcript	3	181438216	cg05513806	S_Shore	Body	22
3	*ARHGEF4***	Rho guanine nucleotide exchange factor (GEF) 4	2	131792772	cg13024709	Island	Body	20
4	*RAPGEFL1***	Rap guanine nucleotide exchange factor (GEF)-like 1	17	38347603	cg20668644	Island	Body	19
				38347968	cg24903006	S_Shore	Body	19
				38347710	cg00129651	Island	Body	14
5	*GRK7**	G protein-coupled receptor kinase 7	3	141516705	cg25640519	S_Shore	Body	18
6	-		2	200327334	cg07835424	Island	-	18
7	-		2	119607885	cg09385093	Island	-	18
8	*KCNA3**	Potassium voltage-gated channel, shaker-related subfamily, member 3	1	111217194	cg20302133	Island	1stExon	15
9	*BCAT1**	Branched chain amino-acid transaminase 1, cytosolic	12	25055967	cg20399616	Island	Body	14
10	*KLF16**	Kruppel-like factor 16	19	1857004	cg04998634	Island	Body	14
11	-		1	170630558	cg23089825	Island	-	14

NOTE: [a]Incidence of frequency of hypermethylation (βvalue > 0.5) in 28 ESCCs. **Primers for HRMA were successfully designed. *Primers for HRMA could not be designed.

doi: 10.1371/journal.pone.0082302.t001

alterations (gain or loss) were defined as more than a 1.5-fold increase or less than a 0.67-fold decrease.

Pathological Analysis of Fraction of Cancer Cells

From paraffin-embedded surgical specimens, serial slice sections with 3-μm thickness were prepared. One section was stained with hematoxylin-eosin, and the remaining sections were used for DNA extraction. An experienced pathologist (R. K.) estimated the fraction of cancer cells by microscopic examination.

Statistical Analyses

The correlation between the fraction of cancer cells estimated by the fraction marker and that assessed by the pathologist was analyzed using Pearson's product-moment correlation coefficients. A difference in the mean fractions of cancer cells was analyzed by Student's t test, and the difference in the variances of the cancer cell fraction was analyzed by Levene's test. All the analyses were performed using PASW statistics version 18.0 (SPSS Japan Inc., Tokyo, Japan), and the results were considered significant when p values <0.05 were obtained by a two-sided test.

Results

Selection of Specific Regions by Genome-wide Screening

Genome-wide methylation analysis was performed using DNA of i) 28 ESCCs obtained by endoscopic biopsy, ii) four ESCC cell lines (KYSE30, KYSE50, KYSE220, and KYSE270), iii) peripheral leukocytes of one healthy volunteer, iv) a pool of normal esophageal mucosae of four healthy volunteers, and v) a pool of non-cancerous esophageal mucosae of eight ESCC patients. We searched for CpG sites that were highly methylated (β value > 0.8) in all the four ESCC cell lines and hardly methylated (β value < 0.1) in peripheral leukocytes, the pool of normal mucosae, and the pool of non-cancerous mucosae, and isolated 2,752 CpG sites from 470,870 informative CpG sites. From the 2,752 CpG sites, we selected 14 CpG sites in which the incidence of hypermethylation (β value > 0.5) in the 28 ESCCs was more than 50% (Figure 1B).

The 14 CpG sites were derived from 11 genomic regions, which we defined as regions within 500bp for convenience (Table 1). From the 11 genomic regions, we excluded *SOX2OT*, which was reported to be highly amplified in ESCC cells [24], and three regions without known genes. For the seven remaining regions, we attempted to design primers for MS-HRMA, which is known as a sensitive and specific method to assess DNA methylation levels [25]. We were able to design primers for three regions (*TFAP2B*, *ARHGEF4*, and *RAPGEFL1*) (Figure 1C).

Qualification of the Three Regions as a Fraction Marker

To confirm that the three regions were completely unmethylated in non-cancerous cells, and completely methylated in cancer cells, we analyzed their methylation levels in i) eight LCM-purified non-cancer cell samples from eight ESCCs, ii) eight LCM-purified cancer cell samples from the eight ESCCs, iii) the eight ESCCs before LCM, iv) peripheral leukocytes of one healthy volunteer, and v) the four ESCC cell lines (Figure 2A).

In the eight LCM-purified non-cancer cell samples and the peripheral leukocytes, all three regions were almost completely unmethylated, and in the four ESCC cell lines, all of them were completely methylated. In the eight LCM-purified cancer cell samples, at least one of the three regions was almost completely methylated. However, *TFAP2B* in sample Et5T, *ARHGEF4* in Et1T, Et2T, Et4T, and Et5T, and *RAPGEFL1* in

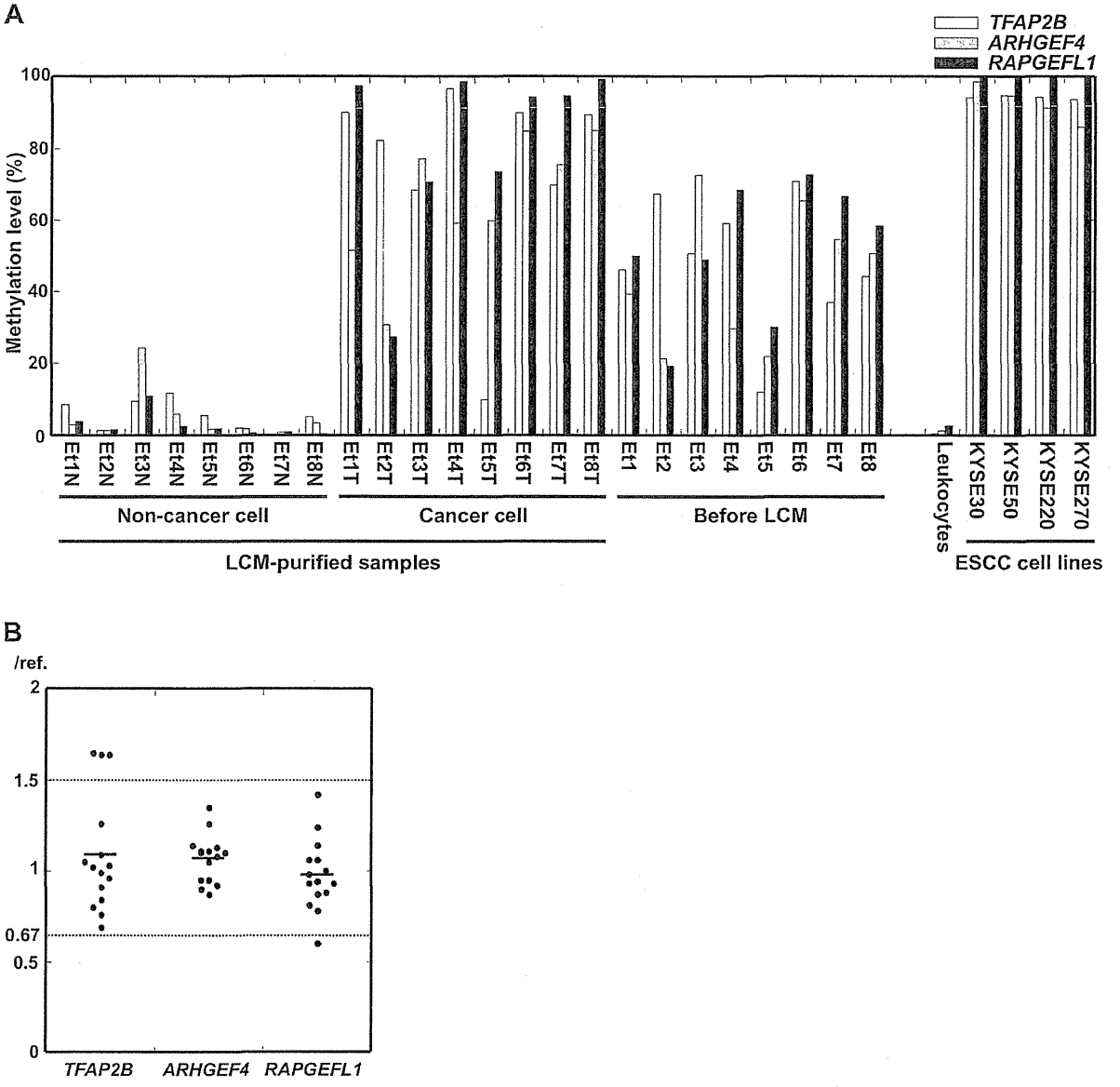

Figure 2

Figure 2. Qualification of the three regions as a fraction marker. (A) Methylation levels of the three regions were analyzed in i) eight LCM-purified non-cancer cell samples from three ESCCs, ii) eight LCM-purified cancer cell samples from the three ESCCs, iii) the eight ESCCs before LCM, iv) peripheral leukocytes of one healthy volunteer, and v) four ESCC cell lines. One or more of the three regions were almost completely methylated in purified cancer cells and cancer cell lines, and all were hardly methylated in non-cancer cells. (B) Copy number alterations of the three regions were analyzed by quantitative PCR using 15 ESCCs.

doi: 10.1371/journal.pone.0082302.g002

Et2T were not completely methylated, possibly due to heterogeneity among cancer cells. Such regions were not suitable as a fraction marker for some specific samples. At the same time, the region with the highest methylation level in the LCM-purified cancer cell samples also showed the highest methylation level in the ESCCs before LCM. Therefore, the

highest methylation level of the three regions was considered to reflect the fraction of cancer cells in the ESCCs.

The methylation level of a region in a sample can be affected by a copy number alteration of the region. Therefore, we analyzed copy number alterations of the three regions using 15 ESCCs (Figure 2B). For *ARHGEF4*, no significant copy number alterations were observed. In contrast, for *TFAP2B* and *RAPGEFL1*, significant copy number alterations were observed at low frequencies (*TFAP2B*, 1.64-1.65 fold changes in three of the 15 ESCCs; *RAPGEFL1*, 0.60-fold change in one of the 15 ESCCs). Assuming that 2-fold or 0.5-fold copy number alterations were present in cancer cells, a deviation of the measured methylation level from the true fraction of cancer cells was calculated to be less than 17.2% (Figure S1). Also, the incidence of significant copy number alterations of *TFAP2B* and *RAPGEFL1* was low (*TFAP2B*, 20%; *RAPGEFL1*, 6.7%). Therefore, the effect of the copy number alterations of *TFAP2B*, and *RAPGEFL1* was considered to be minimal in the estimation of a fraction of cancer cells. Finally, we defined the fraction of cancer cells as the highest methylation level of the three regions.

Analysis of the Accuracy of the Fraction Marker

We then analyzed whether the cancer cell fraction estimated by the fraction marker really reflected the fraction of cancer cells estimated by microscopic examination. We measured methylation levels of the three regions in 20 ESCCs (Figure 3A), and estimated the fraction of cancer cells in each sample, using the highest value of the three regions. In the 20 ESCCs, *TFAP2B*, *ARHGEF4*, and *RAPGEFL1* showed the highest values in nine, nine, and two samples, respectively. Independently, the fraction of cancer cells was estimated by microscopic examination of serial sections. We were able to observe a good correlation between the two methods ($r=0.85$; $p<0.001$) (Figure 3B). This result confirmed that the fraction of cancer cells estimated by the fraction marker accurately reflected the true fraction of cancer cells in a tumor sample.

Application of the Fraction Marker

We applied the fraction marker to compare the fractions of cancer cells between biopsy samples and surgical specimens. The fractions of cancer cells in 39 biopsy samples and 96 surgical specimens were assessed using the fraction marker. Among the 135 samples, *TFAP2B*, *ARHGEF4*, and *RAPGEFL1* had the highest values in 60, 37, and 38 samples, respectively, and the highest values were defined as the fractions of cancer cells in the samples. The mean fraction of cancer cells in the biopsy samples (mean±SD, 53.5±17.1%; range, 7.3-86.7%) was not significantly different from that in the surgical specimens (56.7±18.9%; 14.0-87.3%) ($p=0.377$) (Figure 4A). The variances were large in both the biopsy samples and in the surgical specimens, and there was no significant difference between the biopsy samples and surgical specimens ($p=0.076$). This confirmed that contamination of normal cells must be taken care of for analysis of tumor DNA samples with unknown cancer cell contents.

The fraction marker was also applied to exclude the effect of contamination of normal cells in DNA methylation analysis. For this purpose, we selected CpG sites within 200 bp from transcription start sites (TSS200) for two tumor-suppressor genes (cg22879515 (*MIR34B*) [26], and cg23180938 (*CDO1*) [27]), and assessed distributions of their β values obtained in the initial genome-wide methylation analysis. CpG sites in TSS200 of tumor-suppressor genes were used since they were expected to have no or complete methylation in cancer samples because of the growth advantage conferred by their methylation. The βvalues of the two CpG sites were less than 0.1 in the peripheral leukocytes, the pool of normal mucosae, and the pool of non-cancerous mucosae, and the two CpG sites were considered to be almost completely unmethylated in normal cells. Raw β values of the two CpG sites and βvalues corrected for the cancer cell content [Corrected β value = β value/(a fraction of ESCC cells in the sample (%)/100)] were then compared (Figure 4B). Using the β values corrected by the fraction marker, some samples showed complete methylation (β value ≥ 0.8), some samples showed almost no methylation (β value < 0.2). This result suggested that by using the fraction marker, we were able to minimize the effect of contamination of normal cell DNA in tumor DNA samples for methylation analysis.

Discussion

In this study, the fraction of cancer cells in an ESCC sample was successfully estimated using DNA methylation levels as a fraction marker. To achieve this, we isolated three genomic regions (*TFAP2B*, *ARHGEF4*, and *RAPGEFL1*) that were highly and frequently methylated in ESCC cells, but not in normal cells, by genome-wide methylation analysis. This is the first study in which a fraction of cancer cells in a tumor DNA sample was estimated using DNA methylation. Recently, differentially methylated genomic regions between cancer and normal cells have been identified in many types of cancers [14-18]. Therefore, we can expect to identify specific genomic regions highly and frequently methylated in in the other types of cancer cells, but not in normal cells. By measuring DNA methylation levels of such specific genomic regions, the fraction of cancer cells can be also estimated in DNA samples of other types of cancers.

The accuracy of the fraction marker was verified by comparing the fraction of cancer cells estimated by the fraction marker with that estimated by microscopic examination. A high accuracy was supported by a good correlation between the fractions of cancer cells estimated by the two methods ($r=0.85$). Also, the methylation levels of two CpG sites in TSS200 of two tumor-suppressor genes (*MIR34B* and *CDO1*) were corrected, and some cancer samples showed almost complete methylation. Scatter plot analysis of the β values before and after the correction showed that some of the samples with low β values had large increases (Figure S2). Practically, our fraction marker has the advantage over microscopic examination because it can be used for samples only with DNA and the dedication of experienced pathologists is not necessary. Our fraction marker also has an advantage over approaches using SNP microarray and NGS because it can be used even without paired normal samples, and can be

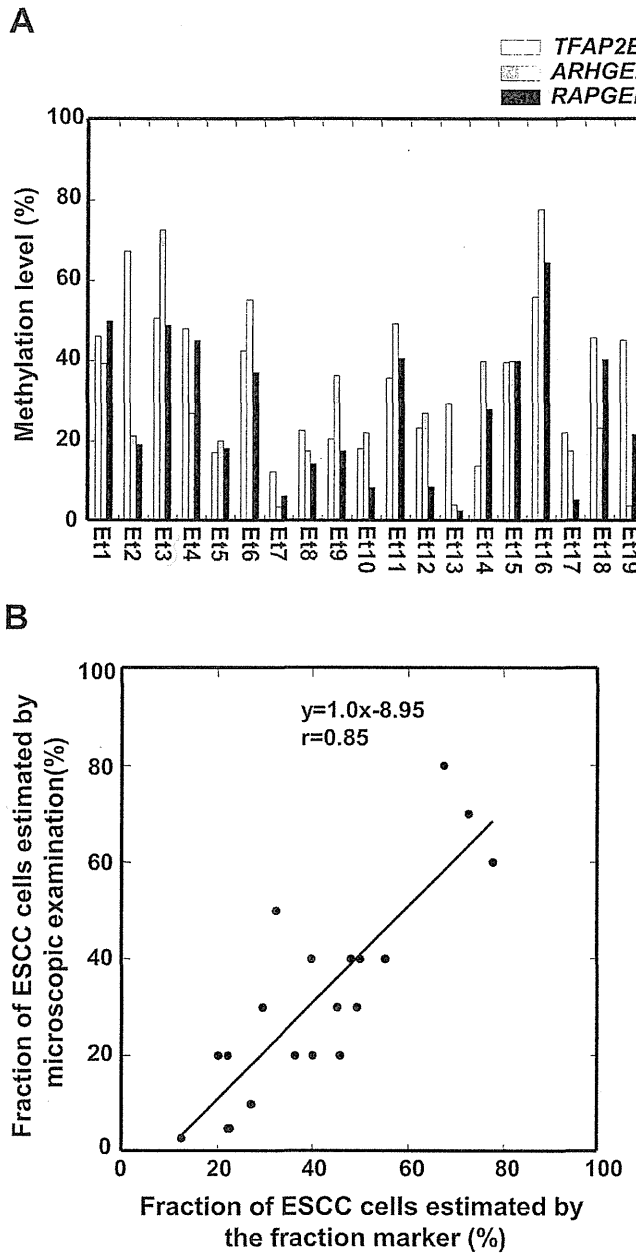

Figure 3

Figure 3. Analysis of the accuracy of the fraction marker. (A) Methylation levels of the three regions were analyzed in 20 ESCCs by MS-HRMA. The fraction of cancer cells in each sample was defined as the highest methylation level of the three regions. (B) Correlation between the fraction of cancer cells estimated by the fraction marker and that assessed by microscopic examination. The correlation between the two methods, calculated using Pearson's product-moment correlation coefficient, was sufficiently high (r=0.85).

doi: 10.1371/journal.pone.0082302.g003

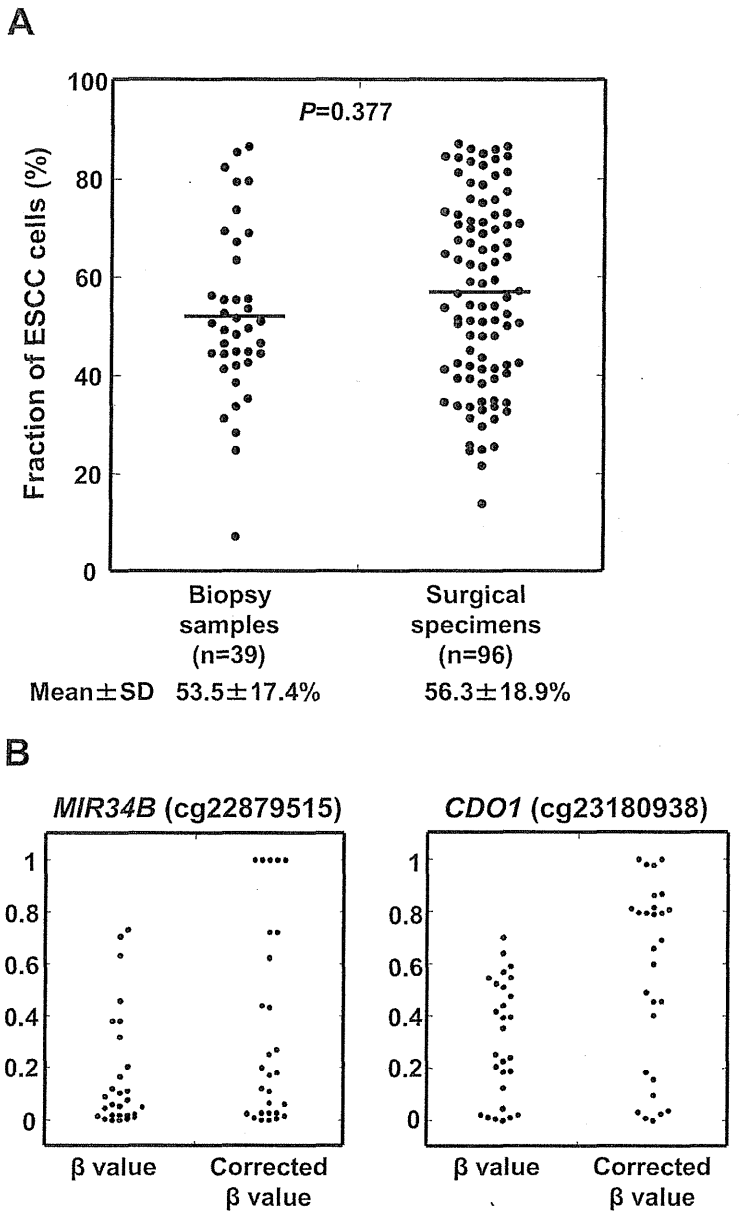

Figure 4

Figure 4. Application of the fraction marker. (A) Application of the fraction marker to comparison of the fraction of cancer cells between biopsy samples and surgical specimens. Fractions of cancer cells in 39 biopsy samples and 96 surgical specimens were estimated by the fraction marker, and no significant difference was observed. (B) Application of the fraction marker to DNA methylation analysis. Raw β values of two CpG sites [cg22879515 (MIR34B), cg23180938 (CDO1)] were corrected by the cancer cell content in 28 ESCCs. Some ESCCs had almost complete methylation (β value ≥ 0.8).

doi: 10.1371/journal.pone.0082302.g004